

Effect of magnesium doping on the orbital and magnetic order in LiNiO_2

M. Bonda,^{1,*} M. Holzapfel,¹ S. de Brion,^{1,2,†} C. Darie,² T. Fehér,^{3,4} P. J. Baker,⁵ T. Lancaster,⁵
S. J. Blundell,⁵ and F. L. Pratt⁶

¹Grenoble High Magnetic Field Laboratory, CNRS, Boîte Postale 166-38042, Grenoble cedex 9, France

²Institut Néel/CNRS-UJF, Boîte Postale 166-38042, Grenoble cedex 9, France

³École Polytechnique Fédérale, Lausanne CH-1015, Switzerland

⁴Condensed Matter Physics Research Group of the HAS and Institute of Physics,

Budapest University of Technology and Economics, P.O. Box 91, H-1521 Budapest, Hungary

⁵Clarendon Laboratory, University of Oxford, Parks Road, Oxford OX1 3PU, United Kingdom

⁶ISIS Muon Facility, ISIS, Chilton, Oxon OX11 0QX, United Kingdom

(Received 14 March 2008; revised manuscript received 23 May 2008; published 16 September 2008; corrected 25 September 2008)

In LiNiO_2 , the Ni^{3+} ions, with $S=1/2$ and twofold orbital degeneracy, are arranged on a triangular lattice. Using muon-spin relaxation and electron-spin resonance (ESR), we show that magnesium doping does not stabilize any magnetic or orbital order despite the absence of interplane Ni^{2+} . A disordered, slowly fluctuating state develops below 12 K. In addition, we find that magnons are excited on the time scale of the ESR experiment. At the same time, a g factor anisotropy is observed, in agreement with $|3z^2-r^2\rangle$ orbital occupancy.

DOI: 10.1103/PhysRevB.78.104409

PACS number(s): 76.75.+i, 75.50.Ee, 76.30.Fc, 76.50.+g

I. INTRODUCTION

Orbital physics in oxides has attracted considerable interest thanks to the discovery of high-temperature superconductivity in cuprates and colossal magnetoresistance in manganites.¹ These macroscopic properties are based on strong correlations between charge, orbital, and magnetic degrees of freedom. In this context, numerous studies have been performed on the orbital and magnetic orders in the isostructural and notionally isoelectronic compounds LiNiO_2 ,²⁻⁴ NaNiO_2 ,^{3,5-9} and more recently AgNiO_2 .¹⁰⁻¹² These compounds offer the possibility of studying a triangular lattice of Ni^{3+} ions with spin $S=1/2$ and twofold orbital degeneracy (e_g orbitals). In NaNiO_2 and AgNiO_2 , it has been possible to characterize both the orbital and magnetic ground states. However in LiNiO_2 , these remain a matter of debate.

The octahedral oxygen crystal field at the Ni^{3+} ions lowers the original spherical $\text{SO}(3)$ symmetry of the Coulomb field and lifts partially the orbital degeneracy, leaving the threefold t_{2g} orbitals lower in energy than the e_g orbital doublet. In NaNiO_2 , the Jahn-Teller (JT) effect further lifts the orbital degeneracy, giving rise to a ferro-orbital ordering of the $|3z^2-r^2\rangle$ orbitals.⁷ In AgNiO_2 , charge transfer occurs $3e_g^1 \rightarrow e_g^2 + e_g^{0.5} + e_g^{0.5}$ with an associated charge ordering.^{10,11} This process removes the orbital degeneracy. In LiNiO_2 , there is no experimental evidence for long-range orbital ordering. Evidence for a dynamic JT effect¹³ has been reported while an extended x-ray-absorption fine structure (EXAFS) study¹⁴ at room temperature concluded rather that $|3z^2-r^2\rangle$ orbitals are occupied. More recently, this orbital occupancy with no long-range orbital order has been confirmed by a neutron-diffraction study.⁴

Magnetic ordering is affected by orbital ordering. In NaNiO_2 , a long-range antiferromagnetic order is observed below 20 K (Refs. 5, 7, 8, 15, and 6) although the proposed A-type magnetic structure (ferromagnetic layers ordered antiferromagnetically) cannot account for all the observed magnetic excitations.⁹ AgNiO_2 shows a more complex antiferro-

magnetic order¹⁰⁻¹² due to different charges on the nickel ions: the Ni^{2+} ($S=1$) sublattice is arranged in ferromagnetic rows ordered antiferromagnetically while the two other nickel sites carry small magnetic moments ($\leq 0.1\mu_B$). Surprisingly, no long-range magnetic order is present in LiNiO_2 . The magnetic ground state has variously been described as a frustrated antiferromagnet,¹⁷ a spin glass,¹⁸ and a disordered quantum state.¹⁹

It must be emphasized that, contrary to NaNiO_2 and AgNiO_2 , LiNiO_2 is never stoichiometric and this may affect the magnetic ground state: Núñez-Regueiro *et al.*²⁰ have shown that the presence of extra Ni^{2+} ions in the Li layers induces a ferromagnetic coupling between the triangular planes that competes with the main antiferromagnetic coupling, leading to magnetic frustration. It may also affect the orbital order since it also generates JT-inactive Ni^{2+} ions in the Ni^{3+} layers.²¹ So how would a pure LiNiO_2 sample behave? To address this issue, we have investigated magnesium-doped LiNiO_2 , which is $\text{LiMg}_x\text{Ni}_{1-x}\text{O}_2$. Doping with magnesium is expected to stabilize the lithium ions on their crystallographic sites and thus to prevent insertion of nickel ions in lithium layers.²² In this paper, we discuss muon-spin-relaxation (μSR) and electron-spin-resonance (ESR) measurements performed to investigate the magnetic and orbital orders of magnesium-doped LiNiO_2 . A comparison with quasistoichiometric LiNiO_2 is presented.

II. SAMPLE CHARACTERIZATION

Powder samples were synthesized using the procedure described by Pouillier *et al.*²² for $\text{LiMg}_x\text{Ni}_{1-x}\text{O}_2$ and by Bianchi *et al.*²³ for LiNiO_2 . X-ray-diffraction patterns were collected using a Siemens 5000 diffractometer. Structural refinement using the Rietveld method was performed with the FULLPROF program. All the samples crystallize in a rhombohedral structure (space-group $R\bar{3}m$) with Ni^{3+} ions occupying the $3b(0,0,1/2)$ site and Li^+ ions the $3a(0,0,0)$ site. The crystal structure can be imagined as an alternating stack-

TABLE I. Room-temperature crystallographic parameters of the $R\bar{3}m$ structure and magnetic parameters of the Curie-Weiss law for quasistoichiometric and Mg-doped LiNiO_2 .

	LiNiO ₂	LiMg _x Ni _{1-x} O ₂		
		$x=0.02$	$x=0.05$	$x=0.10$
Cell param.	$a=2.8728$	$a=2.8724$	$a=2.8734$	$a=2.8773$
(Å)	$c=14.184$	$c=14.187$	$c=14.1978$	$c=14.2245$
θ_{CW}	+29 K	+23.5 K	+22 K	+22 K
θ_{CW} per Ni	+29 K	+24 K	+23 K	+24.5 K
μ_{eff} per Ni	$2.1\mu_{\text{B}}$	$2.1\mu_{\text{B}}$	$2.1\mu_{\text{B}}$	$2.0\mu_{\text{B}}$

ing of lithium and nickel slabs¹⁴ with edge-sharing oxygen octahedra. Nickel ions are arranged on a triangular lattice. Oxygen ions form an octahedron around nickel sites that is responsible for lifting the orbital degeneracy via the crystal field. The Rietveld refinements confirm that the samples are deficient in lithium. In LiNiO_2 , Ni^{2+} replaces Li^+ .²³ In $\text{LiMg}_x\text{Ni}_{1-x}\text{O}_2$, the detailed study by Pouillier *et al.*²² has shown that, for $x \geq 0.2$, only Mg^{2+} replaces Li^+ . This is in agreement with our x-ray data as well as our magnetic-susceptibility data (see below). The resultant nonstoichiometry in the Ni layers has been described in Refs. 23 and 22.

Structural and magnetic properties of the samples studied are presented in Table I. Magnetic susceptibility measurements $\chi(T)$ were performed in a 1 T magnetic field in the temperature range 4–300 K [Fig. 1(a)]. All samples present a Curie-Weiss behavior $\chi(T) = C/(T - \theta_{\text{CW}})$ at high temperature with $\theta_{\text{CW}} > 0$ revealing dominant ferromagnetic interactions (see Table I). The effective magnetic moment deduced from the slope C remains close to $2.0\mu_{\text{B}}$ per Ni ion. The Curie-Weiss temperature θ_{CW} in $\text{Li}_{1-x}\text{Ni}_{1+x}\text{O}_2$ is a linear function of the off stoichiometry:²³ it extrapolates to $\theta_{\text{CW}} = +24$ K for $x=0$ and can be used to determine x ; $x=0.01$ in our sample. For the magnesium-doped samples, the Curie-Weiss tem-

perature is scarcely affected by the number of Mg ions. It is also quite close to the value expected for pure LiNiO_2 and is reduced compared to our LiNiO_2 . This is a confirmation that the additional ferromagnetic interaction present in nonstoichiometric LiNiO_2 is absent in magnesium-doped LiNiO_2 . This makes these samples particularly interesting to determine the orbital and magnetic ground states of pure LiNiO_2 .

Magnetization measurements were performed at 4.2 K in magnetic fields up to 23 T [Fig. 1(b)]. Here also a common behavior for all the samples is observed: a smooth increase in the magnetization and absence of saturation as in a spin glass. This is the same behavior as in quasistoichiometric LiNiO_2 . In the following, we present μSR and ESR results obtained on 5% Mg-doped samples together with those on quasistoichiometric LiNiO_2 .

III. MUON-SPIN-RELAXATION RESULTS

Our μSR experiments²⁴ were carried out using the general purpose surface-muon (GPS) instrument at the Paul Scherrer Institute (PSI), Villigen, Switzerland. Spin-polarized positive muons (μ^+ with mean lifetime of $2.2 \mu\text{s}$, momentum of $29 \text{ MeV}/c$, and gyromagnetic ratio of $\gamma_{\mu}/2\pi = 135.5 \text{ MHz T}^{-1}$) were implanted into the bulk of our polycrystalline samples. Dipole field calculations carried out for the structurally similar compound NaNiO_2 suggest that the muon stopping sites are near the oxygen ions that form the octahedra around the Ni^{3+} ions.¹⁶ The muons stop quickly in the samples (within ~ 1 ns) without significant loss of spin polarization and their average spin polarization is measured as a function of time using the asymmetry $A(t)$ of positrons emitted by muons decaying within the sample.

The measured positron asymmetry $A(t)$ was corrected for the nonrelaxing background signal resulting from muons stopping in the cryostat and sample holder, and normalized to unity. The corrected asymmetry $P_z(t)$ is plotted in Fig. 2 for both compounds. It is clear that in both samples there is

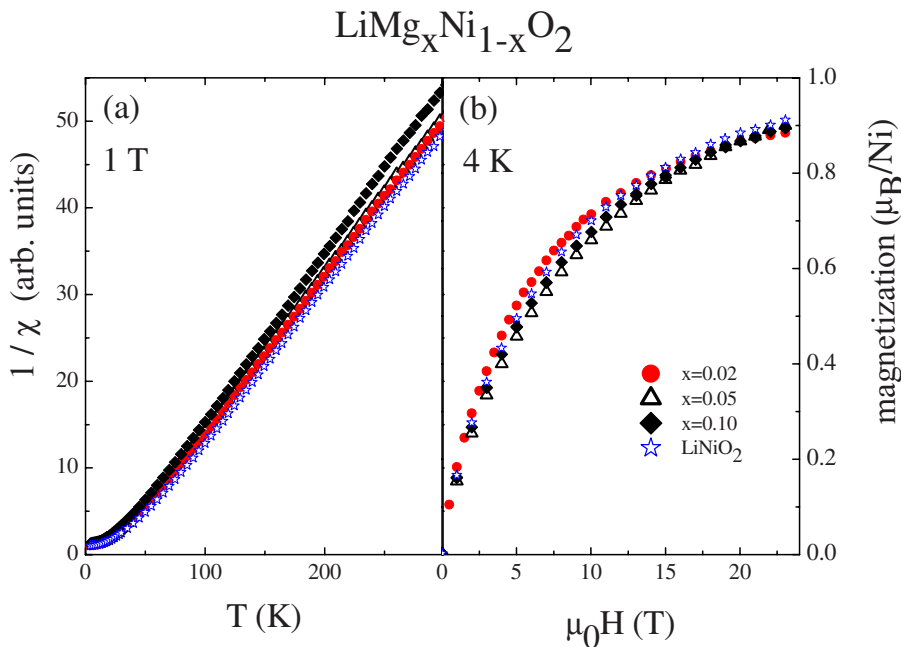


FIG. 1. (Color online) Magnetic properties normalized per Ni ion for quasistoichiometric LiNiO_2 and $\text{LiMg}_x\text{Ni}_{1-x}\text{O}_2$ with $x=0.02$, 0.05, and 0.10. (a) Inverse of the susceptibility at 1 T as a function of temperature. (b) Magnetization at 4 K as a function of magnetic field.

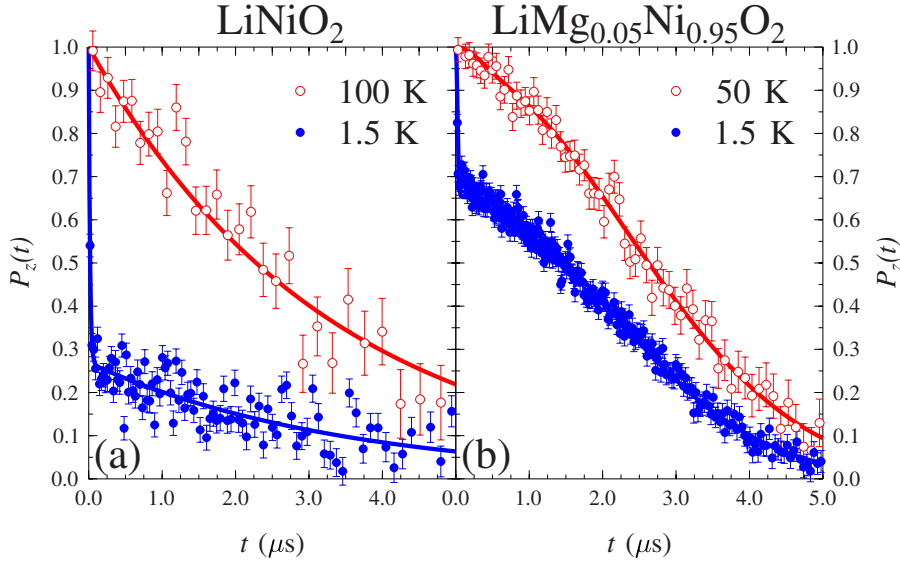


FIG. 2. (Color online) Corrected asymmetry $[P_z(t)]$ data at high and low temperature for: (a) LiNiO_2 with fits to Eq. (1) using the parameters shown in Fig. 3 and (b) 5% Mg-doped sample with fits to Eq. (2) using the parameters shown in Fig. 4. For clarity of display the histogram binning has been altered and the data sets have been normalized with a temperature-independent background subtracted.

no spin precession of the implanted muons, which would give rise to coherent oscillations in the asymmetry spectra. Together with the fact that the high- and low-temperature spectra relax to the same background asymmetry, this is strong evidence for a lack of long-range magnetic order in either sample, as already suggested by the magnetization data (Fig. 1). The form of $P_z(t)$ is sensitive to spin fluctuations on time scales between approximately 10^{-12} and 10^{-4} s.

Examining the data plotted in Fig. 2, we see that in both compounds the low-temperature data is composed of two relaxing components: one with a much higher relaxation rate than the other. The previous μSR study of LiNiO_2 used a stretched exponential $P_z(t) \propto \exp[-(\lambda t)^k]$ to describe the asymmetry data²⁵ but this parametrization was not able to describe our data for either compound over the entire measured temperature range. Two relaxing components were used by Baker *et al.*¹⁶ to describe the muon-spin relaxation at temperatures just above T_N in NaNiO_2 with the amplitude of the fast relaxing component increasing as T_N was approached. Coupled with ac susceptibility measurements, this was taken to be evidence for coalescing magnetic clusters preceding the onset of long-range magnetic order. In both of the present samples, such long-range magnetic order never sets in. The form of the slower relaxing component in each sample is distinguishable, as can be seen in Fig. 2, and is the same at high and low temperatures. We can also see that there is a significant difference in the proportion of the fast and slow relaxing components of the asymmetry between the two samples. This is due to a difference in the quasistatic magnetic volume fraction (see below). We now go on to discuss the results from each sample in turn.

Below approximately 11 K, the asymmetry signal in quasistoichiometric LiNiO_2 is well described by the function:

$$P_z(t) = P_1 e^{-\lambda_1 t} + P_2 e^{-(\sigma_2 t)^2}, \quad (1)$$

where the exponential component describes the slow relaxing component of the signal and the Gaussian component describes the fast relaxation seen at short times (Fig. 2). It is

difficult to resolve the exact form of the fast relaxing component in either sample because the relaxation rate is so large.

At low temperature $P_1 \sim 1/3$ and $P_2 \sim 2/3$, which is the form expected for the relaxation in a polycrystalline sample in the slow-fluctuation (quasistatic) limit. If the sample exhibited long-range magnetic order, P_2 would be multiplied by an oscillating function, as seen in NaNiO_2 (Ref. 16) or AgNiO_2 .¹² The ratio of P_1 and P_2 , and the lack of muon precession suggest that, at low temperature, we have quasistatically disordered magnetic moments throughout the sample. The disorder in the magnetic moments prevents the observation of coherent muon precession. From the size of the Gaussian relaxation rate ($\sigma = \gamma_\mu \Delta B / \sqrt{2}$), we can estimate that the distribution of magnetic fields is approximately $\Delta B \sim 0.5$ T.

It is possible to describe the asymmetry data successfully with Eq. (1) up to around 11 K where we observe a sharp crossover to a regime where the muon-spin relaxation is well described by a single exponential $e^{-\lambda_3 t}$, typical of paramagnetic spin fluctuations when the fluctuation rate is fast compared with the width of the magnetic-field distribution. The crossover is accompanied by a peak in λ , seen in Fig. 3, associated with the slowing down of the electronic fluctuations. Chatterji *et al.*²⁵ found a similar peak in their measured relaxation rate in an applied longitudinal field of 0.6 T, as would be expected if the field has decoupled the muon relaxation due to the quasistatic moments. Their zero-field results²⁵ show a sharp increase in the relaxation rate of the stretched exponential used to parametrize the data below 10 K. The magnitude of the relaxation rate found at low temperature is similar to the value of σ_2 that we found. Parametrizing our data in terms of two separate components [Eq. (1)] allows us to separate these contributions to the muon relaxation in zero applied field. From the magnitude of λ_3 at high temperature, we can estimate the electronic fluctuation rate in the paramagnetic phase to be $\tau = \lambda_3 / 2\gamma_\mu^2 \langle \Delta B^2 \rangle = 32$ ps.

In $\text{LiMg}_{0.05}\text{Ni}_{0.95}\text{O}_2$ the behavior observed is quite similar to the quasistoichiometric LiNiO_2 case. Again we see two

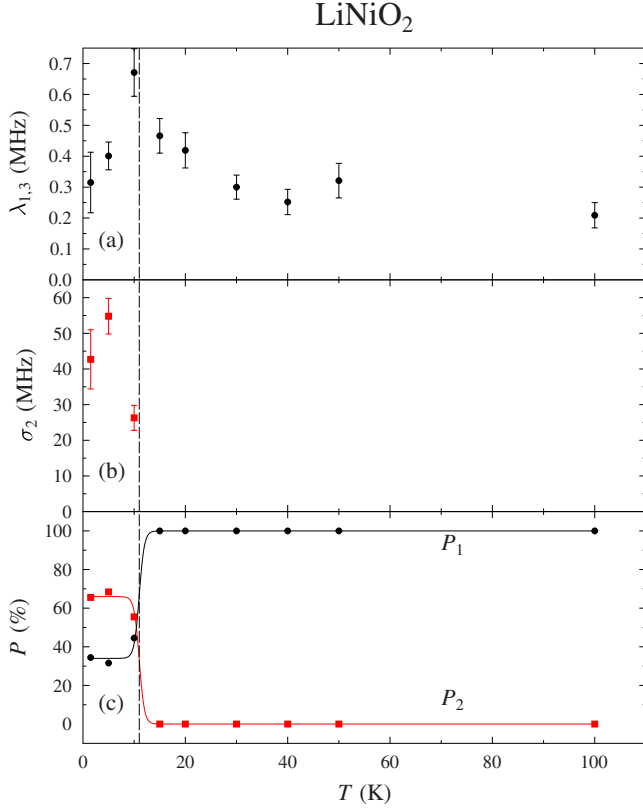


FIG. 3. (Color online) Parameters derived from fitting Eq. (1) to the raw positron asymmetry data for quasistochiometric LiNiO₂. (a) λ_1 and λ_3 describe the slower relaxing component. (b) σ_2 describes the faster relaxing component. (c) Amplitudes of the relaxation components P_1 and P_2 . The lines are guides to the eye.

separate components to the muon-spin relaxation at low temperature but, in this sample, both components take a Gaussian form. This can be described as

$$P_z(t) = P_1 e^{-(\sigma_1 t)^2} + P_2 e^{-(\sigma_2 t)^2}, \quad (2)$$

where we take $\sigma_1 < \sigma_2$. We must consider why the slow relaxing component is Gaussian rather than exponential in this case, as it is also at high temperature. This appears to be due to the motional narrowing of the electronic fluctuations, which are sufficiently fast to leave the muon time window so that the muon is sensitive to the Gaussian distribution of magnetic fields due to randomly orientated nuclear dipoles. This is consistent with the small and almost temperature-independent slow Gaussian relaxation σ_1 plotted in Fig. 4(a). Below ~ 8 K we do not observe a 2:1 ratio in the amplitudes of the two components so the slowly fluctuating region of the sample is not occupying the full sample volume. From the ratio $P_2:P_1$ we can estimate that slowly fluctuating moments occupy approximately three quarters of the sample volume. The μ SR measurements suggest that the electronic moments in the rest of the sample fluctuate sufficiently fast that the slow, temperature-independent relaxation is due to the nuclear moments. The magnitude of σ_2 is similar to that observed in the quasistochiometric sample so the distribu-

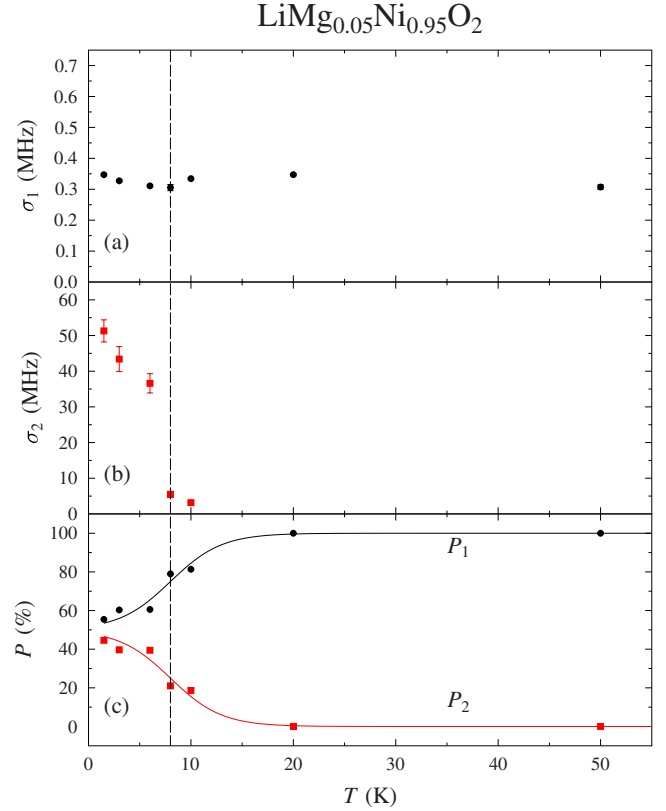


FIG. 4. (Color online) Parameters derived from fitting Eq. (2) to the raw positron asymmetry data for 5% Mg-doped LiNiO₂. (a) σ_1 describes the slower relaxing component. (b) σ_2 describes the faster relaxing component. (c) Amplitudes of the relaxation components P_1 and P_2 . The lines are guides to the eye.

tion of magnetic fields at the muon stopping site is similar, $\Delta B \sim 0.5$ T.

From the μ SR data we can conclude that Mg doping has a significant effect on the spin dynamics of LiNiO₂. While neither sample shows long-ranged magnetic order, as the magnetization data confirms (Fig. 1), the low-temperature state is affected by the presence of the Mg ions. The quasistochiometric sample shows a sharp crossover to a disordered and slowly fluctuating state throughout the sample volume below 12 K. This is accompanied by a peak in the relaxation rate λ_1 , associated with the slowing down of electronic fluctuations. Three-quarters of the volume of the 5% Mg-doped sample enters a similar ground state at low temperature. The remaining part fluctuates too fast to be detectable, and only the nuclear origin of the muon depolarization is observable. Despite the different parametrization, the results of the previous μ SR study²⁵ of Li_{0.98}Ni_{1.02}O₂ appear to be intermediate between those of our doped and undoped samples. Their sample's almost Gaussian high-temperature relaxation is quite similar to that in our 5% Mg-doped sample and the magnitude of the low-temperature relaxation rate is similar to that of the fast relaxing components observed in both of our samples. The 0.6 T longitudinal field measurements give a relaxation rate with a temperature dependence quite similar to the slow relaxing component in our LiNiO₂ sample. This is in agreement with our assignment of

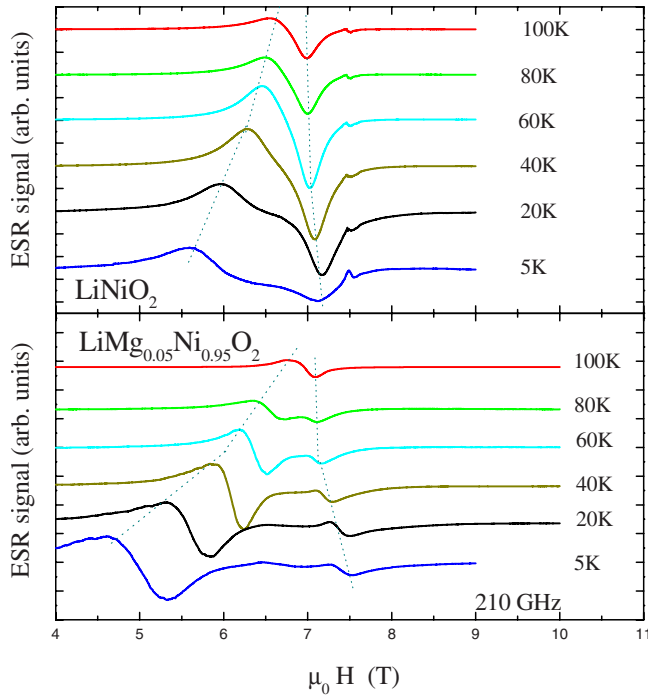


FIG. 5. (Color online) ESR spectra at 210 GHz for quasistoichiometric and Mg-doped LiNiO_2 .

the slow relaxing component to fast fluctuating moments that would not be decoupled by such a field. These comparisons suggest that Chatterji *et al.*'s sample is likely to have had a slightly higher concentration of substitutional defects than our LiNiO_2 sample but lower than our 5% Mg-doped sample.

IV. ELECTRON-SPIN-RESONANCE RESULTS

ESR measurements of magnetic Ni^{3+} ions were carried out over a temperature range of 4–200 K and at three different frequencies, that is, 210, 314, and 420 GHz, using a quasi-optical bridge and a 16 T superconducting magnet. A field modulation was used so that the derivative of the ESR absorption is recorded (Fig. 5).

In highly correlated systems, ESR absorption presents a large linewidth; measuring at high frequencies provides better resolution and also makes it possible to follow magnetic modes up to high magnetic fields. Both the quasistoichiometric and Mg-doped LiNiO_2 samples exhibit a similar ESR response. Three different temperature regimes are observed (see Figs. 5–7). Above about 100 K, the ESR absorption has a Lorentzian line shape; in particular the recorded derivative spectrum is symmetric and its linewidth remains nearly constant for all three frequencies. Below ≈ 100 K, the ESR signal becomes asymmetric and widens with increasing frequency, reflecting some kind of anisotropy, which is crystalline or magnetic in origin. This anisotropy increases dramatically as the temperature is lowered. This is particularly clear in Figs. 6 and 7 where the ESR spectrum total linewidth is plotted as a function of temperature for the three different frequencies. A third temperature regime occurs below about 30 K where the linewidth levels off. Note that the

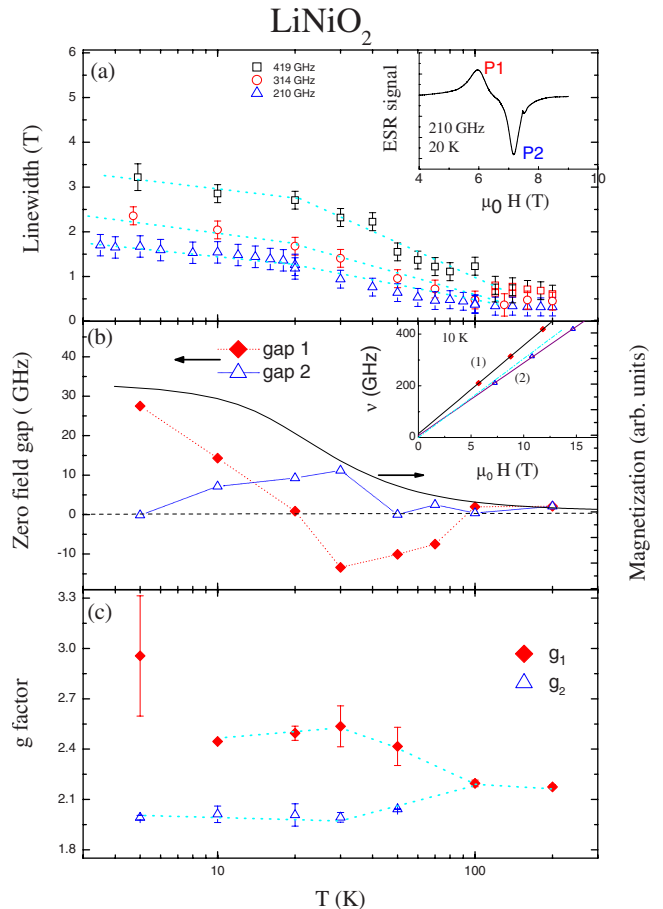


FIG. 6. (Color online) ESR spectra parameters for quasistoichiometric LiNiO_2 as a function of temperature.

ESR spectra are always wider in the Mg-doped sample than in the quasistoichiometric one. Their line shapes at low temperature differ slightly. We will concentrate on the extremal features (peaks P1 and P2), which are similar in both powdered samples.

The question now is to determine the origin of the broadening of the ESR signals with temperature. There are two possibilities. Either it arises from spin-orbital coupling, causing an anisotropy of the g factor when the expected JT effect occurs as observed in NaNiO_2 ,⁷ or it arises from magnetic excitations when some magnetic order is present. Both processes may occur simultaneously. To go further into the analysis, we use a frequency (ν)/magnetic field (H) diagram where the extrema of the ESR spectra are plotted. This procedure enables us to determine the main ESR absorption processes that occur in the powdered samples. Using a linear approximation, we can calculate the corresponding g factors from the high-field slope and the zero-field gaps due to magnetic excitations. This approximation is valid at high fields (see, for instance, Ref. 9). The corresponding frequency/field diagram and linear fit are shown at 5 K in Fig. 6 for quasistoichiometric LiNiO_2 and in Fig. 7 for Mg-doped LiNiO_2 . The light-blue line in the middle is the one calculated for the paramagnetic g factor of free electrons ($g_0=2.0023$, no gap). This linear procedure is then done for several temperatures. As the quality of spectra may vary from one frequency to

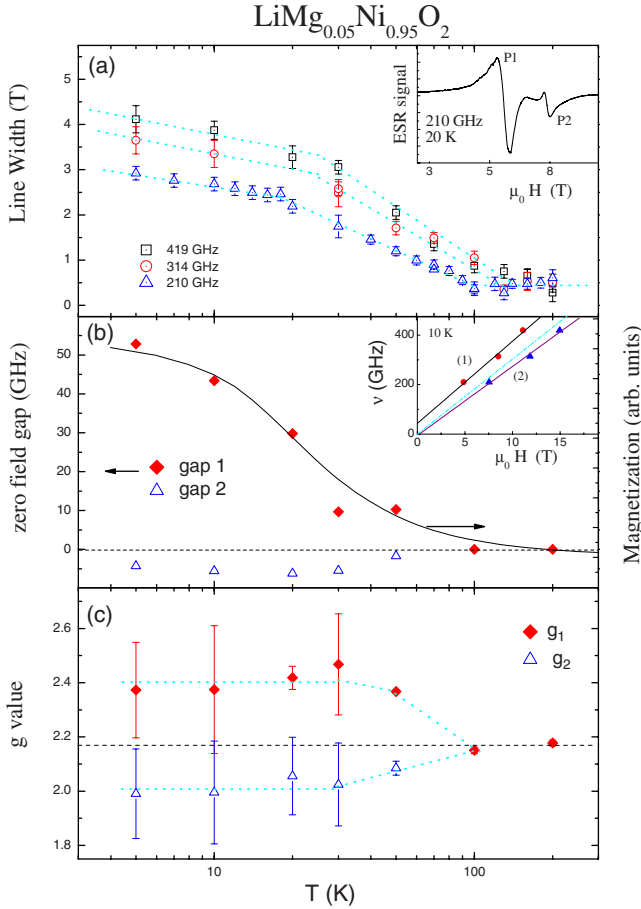


FIG. 7. (Color online) ESR spectra parameters for Mg-doped LiNiO₂ as a function of temperature.

another, error bars may be wide. Above 100 K, the g factor is unique with the same value for both samples quite close to the one derived for the purest LiNiO₂: $g=2.17$.²⁶ While spectra are broadening below 100 K, two distinguishable branches are observed with different g factor and zero-field gap. Below 30 K both g factors stay almost constant while the zero-field gaps continue to vary, at least for Mg-doped LiNiO₂. From this analysis, it is clear that two processes occur simultaneously in both samples: the g factor becomes anisotropic and, at the same time, magnetic excitations develop with a significant zero-field gap for one branch (30–50 GHz at 5 K).

If one assumes a crystallographic origin for the g anisotropy, one can calculate the *effective* g factor of the spin Hamiltonian within perturbation theory applied to the symmetry considered.²⁷ For an elongation of the oxygen octahedra (occupied orbitals $|3z^2-r^2\rangle$),

$$g_{\parallel} = g_0, \quad (3)$$

and

$$g_{\perp} = g_0 - \frac{6\lambda}{\Delta_{cf}}, \quad (4)$$

whereas for a flattening of the octahedra (occupied orbitals $|x^2-y^2\rangle$),

$$g_{\parallel} = g_0 - \frac{8\lambda}{\Delta_{cf}}, \quad (5)$$

and

$$g_{\perp} = g_0 - \frac{2\lambda}{\Delta_{cf}}, \quad (6)$$

where λ is the spin-orbit coupling and Δ_{cf} the crystal-field splitting. Since $\lambda < 0$ for a more than half filled ion as Ni³⁺, we expect $g_{\parallel} < g_{\perp}$ for elongated octahedra and $g_{\parallel} > g_{\perp}$ for flattened octahedra. In a powder spectrum, all the orientations are equally probable, giving rise to a wide spectrum with a particular line shape for each case. It was previously shown that, in NaNiO₂, a powdered spectrum with $g_{\parallel} < g_{\perp}$ is observed at 200 K while a single value of g is observed in LiNiO₂.²⁶ This is confirmed here for our LiNiO₂ sample as well as the Mg-doped sample above 100 K with the same unique value $g=2.17$.

Below ~ 100 K, two different values of g are observed: $g_1=2.0$ and $g_2=2.4$. Since g_1 is equal to g_0 as in the model with occupied ($|3z^2-r^2\rangle$) orbitals, our results are slightly in favor of this model. This is the same orbital occupancy as in NaNiO₂.⁷ However, in the orbital sector, the Li compounds differs from the Na compound in at least two ways. First, in NaNiO₂, there is a ferro-orbital ordering (cooperative JT effect) below 480 K leading to a monoclinic unit cell. In Li compounds, no long-range orbital order is observed: the unit cell remains orthorhombic. Second, for the local-orbital occupancy, it is clear experimentally in NaNiO₂ that the $|3z^2-r^2\rangle$ orbitals are occupied at low temperature.⁷ In Li compounds, the situation is more controversial. An ESR study¹³ suggests that a dynamical Jahn-Teller effect exists that becomes static with $g_{\parallel} > g_{\perp}$ at low temperature and high magnetic field, which means $|3z^2-r^2\rangle$ orbital occupancy. An EXAFS study¹⁴ at room temperature implies the presence of elongated oxygen octahedra around the Ni ions, in agreement with the $|3z^2-r^2\rangle$ orbital occupancy. More recently, a neutron-diffraction and pair density function analysis⁴ concludes that local-orbital order occurs below 375 K with the $|3z^2-r^2\rangle$ orbitals organized in trimers with no long-range order. How can we reconcile all these different results? Note first that our ESR spectra are similar to those observed by Barra *et al.*: a single line at high temperature and a splitted spectrum at low temperature. Our more detailed frequency study shows that the associated g anisotropy corresponds rather to the $|3z^2-r^2\rangle$ orbital occupancy and that there is also an opening of a zero-field gap, which reveals the presence of magnons. Then our results at low temperature are in agreement with the EXAFS and neutron measurements. The single line observed at 200 K arises then from an exchange or a motional mechanism that narrows the g factor anisotropy. For the time scale of the ESR measurements, at the highest frequency, the g anisotropy linewidth can be evaluated at 1.7 T, which corresponds to a characteristic time for the measurement of 20 ps. We conclude that the electronic fluctuation time is temperature dependent with a value smaller than 20 ps above 100 K while below 100 K, it increases to a value longer than 20 ps. From μ SR data in the paramagnetic regime, the electronic fluctuation time is estimated at 32 ps for

LiNiO₂ at 100 K; it is outside the muon time window for the Mg-doped sample at 50 K. These results are quite consistent with those of ESR, assuming that the Mg-doped sample has a higher fluctuating rate. In EXAFS the time scale of the measurement is much shorter, typically 10⁻¹⁵ s so that no narrowing process is observed at room temperature. As for the neutron-diffraction measurements in Ref. 4, we do not know the time scale of the experiment so we cannot conclude further. We propose then the following mechanism: the electrons occupy the $|3z^2-r^2\rangle$ orbitals but the z axis moves. This mechanism is reduced at low temperature at the same time when magnetic excitations are developing (opening of a zero-field gap).

These magnetic excitations are clearly observed in the Mg-doped sample as the progressive opening of a gap for both extremal branches, which follows the sample magnetization (measured at 1 T). The importance of the gap in branch 1 (51 GHz at 4 K) rules out an interpretation with a ferromagnetic origin. Both branches look rather like what is observed in an antiferromagnet. However no long-range magnetic order occurs in this sample, as seen from the magnetization and muon measurements. This means that the time scale on which the sample is probed in ESR is sufficiently short to excite collective magnons. Looking at the line shift due to these magnons at 5 K, for instance, in LiMg_{0.05}Ni_{0.95}O₂, 50 GHz for one branch and 5 GHz for the other branch, we get a characteristic time at 2×10^{-11} and 2×10^{-10} s, respectively. This means that the correlation time of the spin fluctuations is longer than these values for magnons to be observed in ESR. In μ SR, if we assume the same dipolar field created by the Ni ions as in NaNiO₂, a precession in the frequency range 10–100 MHz would be expected if the spin-correlation time is longer. This is not the case in our samples.

If we now compare the ESR spectra for each sample, we see that they have the same intrinsic line width (around 0.5 T), as observed with μ SR. The different magnon branches are better defined in the Mg sample (the total line shape takes the form of two quite well separated modes) than in LiNiO₂ (the line shape appears more like a continuous distribution of modes). This may be related to the differences observed in the μ SR data: the quasistatic glassy state in LiNiO₂ gives rise to a large distribution of magnetic modes. The different relaxing phases in the Mg-doped sample may be related to the two main magnetic modes observed in ESR: one is associated with the g_1 value and has the larger ESR signal. It corresponds to the 2/3 statistical weight of the g_\perp contribution in a powder. It gives the quasistatic signal in μ SR. The second one is associated with the g_2 value and corresponds to the 1/3 g_\parallel contribution. It fluctuates too quickly to give a contribution in μ SR. At high temperature, the spins in the parallel and perpendicular directions are coupled via an exchange mechanism that narrows the ESR line, and, at the

same time, pushes the spin-fluctuation rate outside the μ SR time window. In LiNiO₂, this same exchange mechanism occurs at high temperature although probably at a slower rate since the spin contribution is visible in μ SR. At low temperature, the quasistatic state concerns the whole sample as seen in μ SR.

V. CONCLUSION

In conclusion, we have studied a Mg-doped LiNiO₂ sample without interplane Ni ions and compared it to a quasistoichiometric LiNiO₂ sample. Both the magnetization and μ SR data clearly show that the samples do not undergo a transition to long-ranged magnetic order while the ESR data demonstrate the presence of magnetic excitations with a correlation time longer than 10⁻¹¹–10⁻¹⁰ s. This low-temperature state does, however, change with Mg doping. In our quasistoichiometric LiNiO₂ sample, a disordered, slowly fluctuating state develops in the whole sample volume below 12 K. The corresponding antiferromagnetic magnons excited in ESR have a large frequency distribution with a complex temperature dependence. Mg doping leads to faster electronic fluctuations and smaller slowly fluctuating volume for μ SR. The antiferromagnetic magnons in ESR are better defined and the largest spin gap follows the macroscopic magnetization. In the low-temperature state, both compounds present an anisotropy of the g factor in agreement with the $|3z^2-r^2\rangle$ orbital occupancy with $g_\parallel=2.0$ and $g_\perp=2.4$. A motional narrowing process occurs at the same time when the magnetic excitations disappear, independent of the Mg doping. From this study, it is clear that interplane Ni ions alter the magnetic properties of LiNiO₂ but its removal and replacement by Mg is not sufficient to allow the establishment of long-range magnetic order. In addition, we have shown that both compounds have a single orbital occupancy, as in NaNiO₂, but an exchange mechanism correlated with the magnetic interactions produces dynamical effects above 100 K.

ACKNOWLEDGMENTS

Part of this work was performed at the Swiss Muon Source, Paul Scherrer Institute, Villigen, Switzerland. We thank Alex Amato for technical assistance. T.L. acknowledges support from the Royal Commission of 1851, and T.F. from the Hungarian OTKA PF-63954, K-68807, and Janos Bolyai Research Scholarship of the HAS. We wish to acknowledge Bálint Náfrádi for helping us with the ESR experiments and László Forró from the Swiss Federal Institute of Technology in Lausanne, Switzerland for gratefully providing the ESR experimental setup. The Grenoble High Magnetic Field Laboratory is associated with the Université Joseph Fourier-Grenoble I.

*Present address: École Polytechnique Fédérale, Lausanne CH-1015, Switzerland.

†sophie.debrion@grenoble.cnrs.fr

- ¹Y. Tokura and N. Nagaosa, *Science* **288**, 462 (2000).
- ²J. B. Goodenough, D. G. Wickham, and W. J. Croft, *J. Phys. Chem. Solids* **5**, 107 (1958).
- ³S. de Brion, M. D. Núñez-Regueiro, and G. Chouteau, in *Frontiers in Magnetic Materials*, edited by A. V. Narlikar (Springer Verlag, Berlin, Heidelberg, 2005), pp. 247–272.
- ⁴J.-H. Chung, T. Proffen, S. Shamoto, A. M. Ghorayeb, L. Croguennec, W. Tian, B. C. Sales, R. Jin, D. Mandrus, and T. Egami, *Phys. Rev. B* **71**, 064410 (2005).
- ⁵P. Bongers and U. Enz, *Solid State Commun.* **4**, 153 (1966).
- ⁶E. Chappel, M. D. Núñez-Regueiro, F. Dupont, G. Chouteau, C. Darie, and A. Sulpice, *Eur. Phys. J. B* **17**, 609 (2000).
- ⁷E. Chappel, M. D. Núñez-Regueiro, G. Chouteau, O. Isnard, and C. Darie, *Eur. Phys. J. B* **17**, 615 (2000).
- ⁸M. J. Lewis, B. D. Gaulin, L. Filion, C. Kallin, A. J. Berlinsky, H. A. Dabkowska, Y. Qiu, and J. R. D. Copley, *Phys. Rev. B* **72**, 014408 (2005).
- ⁹S. de Brion, C. Darie, M. Holzapfel, D. Talbayev, L. Mihály, F. Simon, A. Jánossy, and G. Chouteau, *Phys. Rev. B* **75**, 094402 (2007).
- ¹⁰E. Wawrzynska, R. Coldea, E. M. Wheeler, I. I. Mazin, M. D. Johannes, T. Sörgel, M. Jansen, R. M. Ibberson, and P. G. Radaelli, *Phys. Rev. Lett.* **99**, 157204 (2007).
- ¹¹E. Wawrzynska, R. Coldea, E. Wheeler, T. Sörgel, R. I. M. Jansen, P. G. Radaelli, and M. Koza, *Phys. Rev. B* **77**, 094439 (2008).
- ¹²T. Lancaster, S. J. Blundell, P. J. Baker, M. L. Brooks, W. Hayes, F. L. Pratt, R. Coldea, T. Sörgel, and M. Jansen, *Phys. Rev. Lett.* **100**, 017206 (2008).
- ¹³A.-L. Barra, G. Chouteau, A. Stepanov, A. Rougier, and C. Delmas, *Eur. Phys. J. B* **7**, 551 (1999).
- ¹⁴A. Rougier, C. Delmas, and A. Chadwick, *Solid State Commun.* **94**, 123 (1995).
- ¹⁵C. Darie, P. Bordet, S. de Brion, M. Holzapfel, O. I. Lecchi, and E. Suard, *Eur. Phys. J. B* **43**, 159 (2005).
- ¹⁶P. J. Baker, T. Lancaster, S. J. Blundell, M. L. Brooks, W. Hayes, D. Prabhakaran, and F. L. Pratt, *Phys. Rev. B* **72**, 104414 (2005).
- ¹⁷K. Hirota, Y. Nakazawa, and M. Ishikawa, *J. Phys.: Condens. Matter* **3**, 4721 (1991).
- ¹⁸K. Yamaura, M. Takano, A. Hirano, and R. Kanno, *J. Solid State Chem.* **127**, 109 (1996).
- ¹⁹Y. Kitaoka, T. Kobayashi, A. Kōda *et al.*, *J. Phys. Soc. Jpn.* **67**, 3703 (1998).
- ²⁰M. D. N. Chappel, G. Chouteau, and C. Delmas, *Eur. Phys. J. B* **16**, 37 (2000).
- ²¹L. Petit, G. M. Stocks, T. Egami, Z. Szotek, and W. M. Temmerman, *Phys. Rev. Lett.* **97**, 146405 (2006).
- ²²C. Pouillierie, L. Croguenne, P. Biensan, P. Willmann, and C. Delmas, *J. Electrochem. Soc.* **147**, 2061 (2000).
- ²³V. Bianchi, D. Caurant, N. Baffier, C. Belhomme, E. Chappel, G. Chouteau, S. Bach, J. P. Pereira-Ramos, A. Sulpice, and P. Willmann, *Solid State Ionics* **140**, 1 (2001).
- ²⁴S. J. Blundell, *Contemp. Phys.* **40**, 175 (1999).
- ²⁵T. Chatterji, W. Henggeler, and C. Delmas, *J. Phys.: Condens. Matter* **17**, 1341 (2005).
- ²⁶E. Chappel, M. D. Núñez-Regueiro, S. de Brion, G. Chouteau, V. Bianchi, D. Caurant, and N. Baffier, *Phys. Rev. B* **66**, 132412 (2002).
- ²⁷J. A. Ibers and J. D. Swalen, *Phys. Rev.* **127**, 1914 (1962).